

Longitudinal Double-Spin Asymmetry and Cross Section for Inclusive Jet Production in Polarized Proton Collisions at $\sqrt{s} = 200$ GeV

B.I. Abelev,⁵⁰ M.M. Aggarwal,³⁰ Z. Ahammed,⁴⁵ J. Amonett,²⁰ B.D. Anderson,²⁰ M. Anderson,⁶ D. Arkhipkin,¹³ G.S. Averichev,¹² Y. Bai,²⁸ J. Balewski,¹⁷ O. Barannikova,⁹ L.S. Barnby,² J. Baudot,¹⁸ S. Bekele,²⁹ V.V. Belaga,¹² A. Bellingeri-Laurikainen,⁴⁰ R. Bellwied,⁴⁸ F. Benedosso,²⁸ S. Bhardwaj,³⁵ A. Bhasin,¹⁹ A.K. Bhati,³⁰ H. Bichsel,⁴⁷ J. Bielcik,⁵⁰ J. Bielcikova,⁵⁰ L.C. Bland,³ S-L. Blyth,²² B.E. Bonner,³⁶ M. Botje,²⁸ J. Bouchet,⁴⁰ A.V. Brandin,²⁶ A. Bravar,³ T.P. Burton,² M. Bystersky,¹¹ R.V. Cadman,¹ X.Z. Cai,³⁹ H. Caines,⁵⁰ M. Calderón de la Barca Sánchez,⁶ J. Castillo,²⁸ O. Catu,⁵⁰ D. Cebra,⁶ Z. Chajecski,²⁹ P. Chaloupka,¹¹ S. Chattopadhyay,⁴⁵ H.F. Chen,³⁸ J.H. Chen,³⁹ J. Cheng,⁴³ M. Cherney,¹⁰ A. Chikanian,⁵⁰ W. Christie,³ J.P. Coffin,¹⁸ T.M. Cormier,⁴⁸ M.R. Cosentino,³⁷ J.G. Cramer,⁴⁷ H.J. Crawford,⁵ D. Das,⁴⁵ S. Das,⁴⁵ S. Dash,¹⁵ M. Daugherty,⁴² M.M. de Moura,³⁷ T.G. Dedovich,¹² M. DePhillips,³ A.A. Derevschikov,³² L. Didenko,³ T. Dietel,¹⁴ P. Djawotho,¹⁷ S.M. Dogra,¹⁹ W.J. Dong,⁷ X. Dong,³⁸ J.E. Draper,⁶ F. Du,⁵⁰ V.B. Dunin,¹² J.C. Dunlop,³ M.R. Dutta Mazumdar,⁴⁵ V. Eckardt,²⁴ W.R. Edwards,²² L.G. Efimov,¹² V. Emelianov,²⁶ J. Engelage,⁵ G. Eppley,³⁶ B. Erazmus,⁴⁰ M. Estienne,¹⁸ P. Fachini,³ R. Fatemi,²³ J. Fedorisin,¹² P. Filip,¹³ E. Finch,⁵⁰ V. Fine,³ Y. Fisyak,³ J. Fu,⁴⁹ C.A. Gagliardi,⁴¹ L. Gaillard,² M.S. Ganti,⁴⁵ V. Ghazikhanian,⁷ P. Ghosh,⁴⁵ J.E. Gonzalez,⁷ Y.G. Gorbunov,¹⁰ H. Gos,⁴⁶ O. Grebenyuk,²⁸ D. Grosnick,⁴⁴ S.M. Guertin,⁷ K.S.F.F. Guimaraes,³⁷ N. Gupta,¹⁹ T.D. Gutierrez,⁶ B. Haag,⁶ T.J. Hallman,³ A. Hamed,⁴⁸ J.W. Harris,⁵⁰ W. He,¹⁷ M. Heinz,⁵⁰ T.W. Henry,⁴¹ S. Hepplemann,³¹ B. Hippolyte,¹⁸ A. Hirsch,³³ E. Hjort,²² A.M. Hoffman,²³ G.W. Hoffmann,⁴² M.J. Horner,²² H.Z. Huang,⁷ S.L. Huang,³⁸ E.W. Hughes,⁴ T.J. Humanic,²⁹ G. Igo,⁷ P. Jacobs,²² W.W. Jacobs,¹⁷ P. Jakl,¹¹ F. Jia,²¹ H. Jiang,⁷ P.G. Jones,² E.G. Judd,⁵ S. Kabana,⁴⁰ K. Kang,⁴³ J. Kapitan,¹¹ M. Kaplan,⁸ D. Keane,²⁰ A. Kechechyan,¹² V.Yu. Khodyrev,³² B.C. Kim,³⁴ J. Kiryluk,²³ A. Kisiel,⁴⁶ E.M. Kislov,¹² S.R. Klein,²² A. Kocoloski,²³ D.D. Koetke,⁴⁴ T. Kollegger,¹⁴ M. Kopytine,²⁰ L. Kotchenda,²⁶ V. Kouchpil,¹¹ K.L. Kowalik,²² M. Kramer,²⁷ P. Kravtsov,²⁶ V.I. Kravtsov,³² K. Krueger,¹ C. Kuhn,¹⁸ A.I. Kulikov,¹² A. Kumar,³⁰ A.A. Kuznetsov,¹² M.A.C. Lamont,⁵⁰ J.M. Landgraf,³ S. Lange,¹⁴ S. LaPointe,⁴⁸ F. Laue,³ J. Lauret,³ A. Lebedev,³ R. Lednicky,¹³ C-H. Lee,³⁴ S. Lehocka,¹² M.J. LeVine,³ C. Li,³⁸ Q. Li,⁴⁸ Y. Li,⁴³ G. Lin,⁵⁰ X. Lin,⁴⁹ S.J. Lindenbaum,²⁷ M.A. Lisa,²⁹ F. Liu,⁴⁹ H. Liu,³⁸ J. Liu,³⁶ L. Liu,⁴⁹ Z. Liu,⁴⁹ T. Ljubicic,³ W.J. Llope,³⁶ H. Long,⁷ R.S. Longacre,³ W.A. Love,³ Y. Lu,⁴⁹ T. Ludlam,³ D. Lynn,³ G.L. Ma,³⁹ J.G. Ma,⁷ Y.G. Ma,³⁹ D. Magestro,²⁹ D.P. Mahapatra,¹⁵ R. Majka,⁵⁰ L.K. Mangotra,¹⁹ R. Manweiler,⁴⁴ S. Margetis,²⁰ C. Markert,⁴² L. Martin,⁴⁰ H.S. Matis,²² Yu.A. Matulenko,³² C.J. McClain,¹ T.S. McShane,¹⁰ Yu. Melnick,³² A. Meschanin,³² J. Millane,²³ M.L. Miller,²³ N.G. Minaev,³² S. Mioduszewski,⁴¹ C. Mironov,²⁰ A. Mischke,²⁸ D.K. Mishra,¹⁵ J. Mitchell,³⁶ B. Mohanty,⁴⁵ L. Molnar,³³ C.F. Moore,⁴² D.A. Morozov,³² M.G. Munhoz,³⁷ B.K. Nandi,¹⁶ C. Nattrass,⁵⁰ T.K. Nayak,⁴⁵ J.M. Nelson,² P.K. Netrakanti,⁴⁵ L.V. Nogach,³² S.B. Nurushev,³² G. Odyniec,²² A. Ogawa,³ V. Okorokov,²⁶ M. Oldenburg,²² D. Olson,²² M. Pachr,¹¹ S.K. Pal,⁴⁵ Y. Panebratsev,¹² S.Y. Panitkin,³ A.I. Pavlinov,⁴⁸ T. Pawlak,⁴⁶ T. Peitzmann,²⁸ V. Perevoztchikov,³ C. Perkins,⁵ W. Peryt,⁴⁶ S.C. Phatak,¹⁵ R. Picha,⁶ M. Planinic,⁵¹ J. Pluta,⁴⁶ N. Poljak,⁵¹ N. Porile,³³ J. Porter,⁴⁷ A.M. Poskanzer,²² M. Potekhin,³ E. Potrebenikova,¹² B.V.K.S. Potukuchi,¹⁹ D. Prindle,⁴⁷ C. Pruneau,⁴⁸ J. Putschke,²² G. Rakness,³¹ R. Raniwala,³⁵ S. Raniwala,³⁵ R.L. Ray,⁴² S.V. Razin,¹² J. Reinnarth,⁴⁰ D. Relyea,⁴ A. Ridiger,²⁶ H.G. Ritter,²² J.B. Roberts,³⁶ O.V. Rogachevskiy,¹² J.L. Romero,⁶ A. Rose,²² C. Roy,⁴⁰ L. Ruan,²² M.J. Russcher,²⁸ R. Sahoo,¹⁵ T. Sakuma,²³ S. Salur,⁵⁰ J. Sandweiss,⁵⁰ M. Sarsour,⁴¹ P.S. Sazhin,¹² J. Schambach,⁴² R.P. Scharenberg,³³ N. Schmitz,²⁴ J. Seger,¹⁰ I. Selyuzhenkov,⁴⁸ P. Seyboth,²⁴ A. Shabetai,²⁰ E. Shahaliev,¹² M. Shao,³⁸ M. Sharma,³⁰ W.Q. Shen,³⁹ S.S. Shimanskiy,¹² E.P. Sichtermann,²² F. Simon,²³ R.N. Singaraaju,⁴⁵ N. Smirnov,⁵⁰ R. Snellings,²⁸ G. Sood,⁴⁴ P. Sorensen,³ J. Sowinski,¹⁷ J. Speltz,¹⁸ H.M. Spinka,¹ B. Srivastava,³³ A. Stadnik,¹² T.D.S. Stanislaus,⁴⁴ R. Stock,¹⁴ A. Stolpovsky,⁴⁸ M. Strikhanov,²⁶ B. Stringfellow,³³ A.A.P. Suaide,³⁷ E. Sugarbaker,²⁹ M. Sumbera,¹¹ Z. Sun,²¹ B. Surrow,²³ M. Swanger,¹⁰ T.J.M. Symons,²² A. Szanto de Toledo,³⁷ A. Tai,⁷ J. Takahashi,³⁷ A.H. Tang,³ T. Tarnowsky,³³ D. Thein,⁷ J.H. Thomas,²² A.R. Timmins,² S. Timoshenko,²⁶ M. Tokarev,¹² T.A. Trainor,⁴⁷ S. Trentalange,⁷ R.E. Tribble,⁴¹ O.D. Tsai,⁷ J. Ulery,³³ T. Ullrich,³ D.G. Underwood,¹ G. Van Buren,³ N. van der Kolk,²⁸ M. van Leeuwen,²² A.M. Vander Molen,²⁵ R. Varma,¹⁶ I.M. Vasilevski,¹³ A.N. Vasiliev,³² R. Vernet,¹⁸ S.E. Vigdor,¹⁷ Y.P. Viyogi,¹⁵ S. Vokal,¹² S.A. Voloshin,⁴⁸ W.T. Waggoner,¹⁰ F. Wang,³³ G. Wang,⁷ J.S. Wang,²¹ X.L. Wang,³⁸ Y. Wang,⁴³ J.W. Watson,²⁰ J.C. Webb,⁴⁴ G.D. Westfall,²⁵ A. Wetzler,²² C. Whitten Jr.,⁷ H. Wieman,²² S.W. Wissink,¹⁷ R. Witt,⁵⁰ J. Wood,⁷ J. Wu,³⁸ N. Xu,²² Q.H. Xu,²²

Z. Xu,³ P. Yepes,³⁶ I-K. Yoo,³⁴ V.I. Yurevich,¹² W. Zhan,²¹ H. Zhang,³ W.M. Zhang,²⁰ Y. Zhang,³⁸
 Z.P. Zhang,³⁸ Y. Zhao,³⁸ C. Zhong,³⁹ R. Zoulkarneev,¹³ Y. Zoulkarneeva,¹³ A.N. Zubarev,¹² and J.X. Zuo³⁹
 (STAR Collaboration)

- ¹Argonne National Laboratory, Argonne, Illinois 60439
²University of Birmingham, Birmingham, United Kingdom
³Brookhaven National Laboratory, Upton, New York 11973
⁴California Institute of Technology, Pasadena, California 91125
⁵University of California, Berkeley, California 94720
⁶University of California, Davis, California 95616
⁷University of California, Los Angeles, California 90095
⁸Carnegie Mellon University, Pittsburgh, Pennsylvania 15213
⁹University of Illinois, Chicago
¹⁰Creighton University, Omaha, Nebraska 68178
¹¹Nuclear Physics Institute AS CR, 250 68 Řež/Prague, Czech Republic
¹²Laboratory for High Energy (JINR), Dubna, Russia
¹³Particle Physics Laboratory (JINR), Dubna, Russia
¹⁴University of Frankfurt, Frankfurt, Germany
¹⁵Institute of Physics, Bhubaneswar 751005, India
¹⁶Indian Institute of Technology, Mumbai, India
¹⁷Indiana University, Bloomington, Indiana 47408
¹⁸Institut de Recherches Subatomiques, Strasbourg, France
¹⁹University of Jammu, Jammu 180001, India
²⁰Kent State University, Kent, Ohio 44242
²¹Institute of Modern Physics, Lanzhou, China
²²Lawrence Berkeley National Laboratory, Berkeley, California 94720
²³Massachusetts Institute of Technology, Cambridge, MA 02139-4307
²⁴Max-Planck-Institut für Physik, Munich, Germany
²⁵Michigan State University, East Lansing, Michigan 48824
²⁶Moscow Engineering Physics Institute, Moscow Russia
²⁷City College of New York, New York City, New York 10031
²⁸NIKHEF and Utrecht University, Amsterdam, The Netherlands
²⁹Ohio State University, Columbus, Ohio 43210
³⁰Panjab University, Chandigarh 160014, India
³¹Pennsylvania State University, University Park, Pennsylvania 16802
³²Institute of High Energy Physics, Protvino, Russia
³³Purdue University, West Lafayette, Indiana 47907
³⁴Pusan National University, Pusan, Republic of Korea
³⁵University of Rajasthan, Jaipur 302004, India
³⁶Rice University, Houston, Texas 77251
³⁷Universidade de Sao Paulo, Sao Paulo, Brazil
³⁸University of Science & Technology of China, Hefei 230026, China
³⁹Shanghai Institute of Applied Physics, Shanghai 201800, China
⁴⁰SUBATECH, Nantes, France
⁴¹Texas A&M University, College Station, Texas 77843
⁴²University of Texas, Austin, Texas 78712
⁴³Tsinghua University, Beijing 100084, China
⁴⁴Valparaiso University, Valparaiso, Indiana 46383
⁴⁵Variable Energy Cyclotron Centre, Kolkata 700064, India
⁴⁶Warsaw University of Technology, Warsaw, Poland
⁴⁷University of Washington, Seattle, Washington 98195
⁴⁸Wayne State University, Detroit, Michigan 48201
⁴⁹Institute of Particle Physics, CCNU (HZNU), Wuhan 430079, China
⁵⁰Yale University, New Haven, Connecticut 06520
⁵¹University of Zagreb, Zagreb, HR-10002, Croatia

(Dated: December 2, 2024)

We report a measurement of the longitudinal double-spin asymmetry A_{LL} and the differential cross section for inclusive mid-rapidity jet production in polarized proton collisions at $\sqrt{s} = 200$ GeV. The cross section data cover transverse momenta $5 < p_T < 50$ GeV/c and agree with next-to-leading order perturbative QCD (NLO pQCD) evaluations. The spin asymmetry data, presented for jets with $5 < p_T < 17$ GeV/c, disfavor large positive values of gluon polarization in the polarized nucleon.

PACS numbers: 13.88.+e, 12.38.Qk, 13.87.-a, 14.20.Dh, 24.70.+s

Deep-inelastic scattering (DIS) experiments with polarized leptons and polarized nucleons have found that the spins of quarks and anti-quarks account for only about 25% of the nucleon spin [1]. The gluon helicity distribution and orbital angular momenta are thus expected to be essential to the understanding of the nucleon spin. Measurements of the scale dependence of the inclusive nucleon spin structure function [2] and recent semi-inclusive DIS data [3] have coarsely constrained the possible gluon spin contribution. Complementary measurements with strongly interacting probes give sensitivity to gluons via quark-gluon and gluon-gluon scattering contributions [4, 5].

In this paper we report the first measurement of the longitudinal double-spin asymmetry for inclusive jet production in polarized proton collisions,

$$A_{LL} = \frac{\sigma^{++} - \sigma^{+-}}{\sigma^{++} + \sigma^{+-}}, \quad (1)$$

where σ^{++} and σ^{+-} are the inclusive jet cross sections when the two colliding proton beams have equal and opposite helicities, respectively. In addition we report the inclusive jet differential cross section.

In perturbative QCD the (un-)polarized jet cross section involves a convolution of (un-)polarized quark and gluon distribution functions and the (un-)polarized hard partonic scattering cross section [6, 7]. It does not involve fragmentation functions. We compare NLO pQCD calculations with the measured cross section to test their applicability and to support their use in constraining the polarized gluon distribution function through measurement of A_{LL} . The measurements, covering jet transverse momenta $5 < p_T < 50$ GeV/c and jet pseudorapidities $0.2 < \eta < 0.8$, are sensitive to gluon polarization for momentum fractions $0.03 < x < 0.3$.

The data were collected at the Brookhaven Relativistic Heavy Ion Collider (RHIC) with the Solenoidal Tracker at RHIC (STAR) [8] during 3 week beam periods in the years 2003 and 2004. Beam bunches of ~ 1 ns duration with $5-7 \times 10^{10}$ polarized protons of 100 GeV energy crossed the STAR interaction region (IR) every 213 ns. Typical luminosities were $2-5 \times 10^{30}$ cm⁻²s⁻¹. Spin rotator magnets upstream and downstream of the IR rotated the proton beam spins from and to the stable vertical direction in RHIC to provide collisions with longitudinal polarizations [8]. The helicities alternated for successive bunches of one beam and for successive pairs of bunches of the other beam. Thus STAR recorded collisions with all beam helicity combinations in rapid succession.

The degree of polarization was measured for each beam and for each beam fill with RHIC Coulomb-Nuclear Interference (CNI) proton-carbon polarimeters [9], which were calibrated *in situ* using a polarized atomic hydrogen gas-jet target [10]. Proton beam polarizations were 30–45%. Non-longitudinal beam polarization components at

the STAR IR were measured continually with local polarimeters [11] and were no larger than 9% (absolute).

The STAR detector subsystems [8] of principal interest here are the Time Projection Chamber (TPC), the Barrel Electromagnetic Calorimeter (BEMC), and the Beam-Beam Counters (BBC). The TPC provides charged particle tracking in the 0.5 T solenoid magnetic field for all azimuthal angles (ϕ), radii between 0.5 and 2.0 m, and longitudinal positions out to $z = \pm 2.1$ m. Its coverage is thus $|\eta| \lesssim 1.3$. The BEMC is a lead-scintillator sampling calorimeter at 2.3 m radius, covering all ϕ and $0 < \eta < 1$ with respect to the TPC center in 2003 and 2004. The BBCs are composed of segmented scintillator annuli that span $3.3 < |\eta| < 5.0$ and measure the proton beam luminosity and transverse polarization components.

Proton collision events were identified by coincident signals from at least one BBC segment on either side of the IR. The cross section measured for the BBC coincidence requirement is 26.1 ± 2.0 mb, which is 87% of the non-singly diffractive pp cross section [12]. The jet data were collected with a minimum bias (MB) and a high tower (HT) calorimetric trigger condition. The MB trigger required a proton collision event and was highly pre-scaled. The HT trigger required, in addition, a signal from at least one BEMC tower of size $\Delta\eta \times \Delta\phi = 0.05 \times 0.05$ above a transverse energy (E_T) threshold of 2.2 GeV in 2003 (2.2–3.4 GeV at $\eta = 0-1$ in 2004). In total 2.1×10^6 MB and 3.0×10^6 HT events were analyzed. The integrated luminosity $\int \mathcal{L} dt$ amounts to 0.18 (0.12) pb⁻¹ for the analyzed 2003 (2004) data.

Jets were reconstructed using a midpoint-cone algorithm [13] that clusters reconstructed TPC tracks and BEMC energy deposits within a cone of radius $r_{\text{cone}} = 0.4$ in η and ϕ , starting from energy seeds of at least 0.5 GeV. Particle tracks with $p_T > 0.2$ GeV/c were considered if they originated from the primary interaction vertex. The primary interaction vertex was required to be on the beam axis and within $z = \pm 60$ cm to ensure uniform tracking efficiency. Calorimeter towers were considered if their E_T exceeded 0.2 GeV after correction for charged hadron contributions included through TPC tracking. A charged pion (photon) mass was assumed for tracks (towers) in relating energy and momentum. Jets were required to have a reconstructed jet axis intersecting the BEMC at nominal η between 0.2 and 0.8 and a reconstructed jet $p_T > 5$ GeV/c. A minimum TPC contribution to the jet energy, $E_{\text{TPC}}/E_{\text{tot}} > 0.2$ (0.1) in 2003 (2004), was used to suppress apparent jets from beam background. The jet p_T resolution was determined to be $\sim 25\%$ from the momentum balance of di-jet events and from simulation, and motivated the choice of binning.

Figure 1 shows the jet profile $\Psi(\Delta r, r_{\text{cone}}, p_T)$, defined as the average fraction of jet E_T inside a coaxial inner cone of radius $\Delta r < r_{\text{cone}}$, for the MB and HT data separately. The HT trigger, providing increased selectivity for jets, causes a bias toward jets with hard fragments

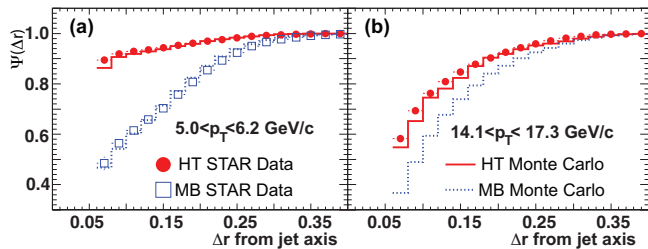


FIG. 1: Jet profile $\Psi(\Delta r, r_{\text{cone}}, p_T)$ versus inner cone size Δr at $r_{\text{cone}} = 0.4$ for MB (open squares) and HT (filled circles) data compared with STAR Monte Carlo simulation in two jet p_T bins (a) $5.0 < p_T < 6.2$ and (b) $14.1 < p_T < 17.3$ GeV/c. The MB jet yield is insufficient in the latter range.

that produce an electromagnetic shower. The distributions, including this p_T dependent trigger bias, are well reproduced by PYTHIA-based (v 6.205 [14] ‘CDF TuneA’ settings [15]) Monte Carlo simulations passed through GEANT-based [16] STAR detector simulation. The reconstruction software imposed the same trigger requirements as in the data. In the cross section analysis of HT data an E_T threshold of 3.5 GeV was imposed on the BEMC trigger tower to ensure a uniform trigger efficiency.

The differential inclusive cross sections were determined separately for the MB and HT data according to

$$\frac{1}{2\pi} \frac{d^2\sigma}{d\eta dp_T} = \frac{1}{2\pi} \cdot \frac{N_{\text{jets}}}{\Delta\eta \Delta p_T} \cdot \frac{1}{\int \mathcal{L} dt} \cdot \frac{1}{c(p_T)}, \quad (2)$$

where N_{jets} denotes the number of jets observed within a pseudo-rapidity interval $\Delta\eta$ and a transverse momentum interval Δp_T at a mean jet p_T . The correction factors $c(p_T)$ were determined from simulation, and are defined as the ratio of the number of jets reconstructed within a given p_T interval in the simulated data to those generated in the PYTHIA final-state particle record. They change monotonically for HT events from 0.02 at $p_T = 8.3$ GeV/c to 0.79 at $p_T = 43$ GeV/c, whereas they are a constant 0.69 for MB events with $p_T < 12.6$ GeV/c. Consistent values were obtained with the HERWIG [17] generator. Typically 35–40% of the jets generated in a given p_T interval were reconstructed in the same interval. Reconstructed p_T was found to be on average larger than generated p_T by a constant $\sim 20\%$ in each reconstructed p_T interval, and the difference is taken into account via $c(p_T)$.

The MB differential cross sections extracted from 1.4×10^3 jets collected in 2003 and 1.1×10^3 in 2004 are in good agreement ($\chi^2/\text{ndf} = 0.8$). A systematic offset of 20%, roughly independent of p_T , was found between the HT differential cross sections extracted from 43×10^3 and 42×10^3 jets collected in 2003 and 2004. We ascribe this difference to a 5% uncertainty in the year-to-year absolute scale of the BEMC calibration and to uncertainty in the modeling of temporary BEMC hardware malfunctions. In 2003 the BEMC was calibrated using 20×10^6 d+Au collision events, whereas 50×10^6 Au+Au events

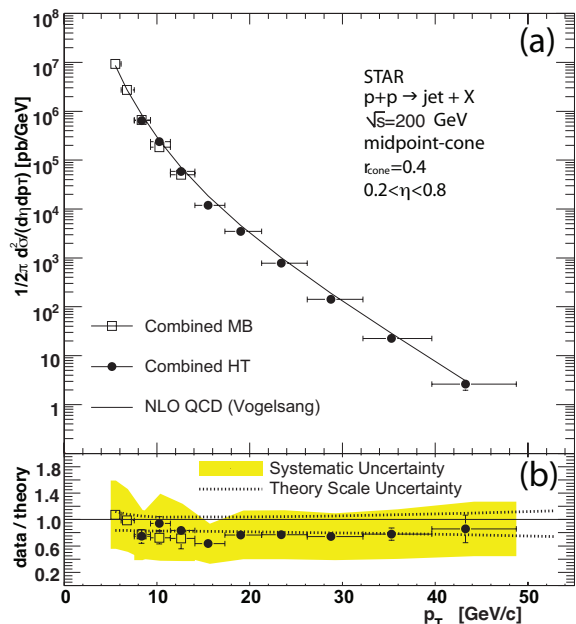


FIG. 2: (a) Inclusive differential cross section for $p+p \rightarrow \text{jet} + X$ at $\sqrt{s} = 200$ GeV versus jet p_T for a jet cone radius of 0.4. The symbols show MB (open squares) and HT (filled circles) data from the years 2003 and 2004 combined. The horizontal bars indicate the ranges of the p_T intervals. The curve shows a NLO calculation [6]. (b) Comparison of theory and data. The band indicates the experimental systematic uncertainty. The upper (lower) dashed line indicates the relative change of the NLO calculation when it is evaluated at $\mu = p_T/2$ ($\mu = 2p_T$).

were used in 2004. The absolute energy scale was set by matching BEMC energy to TPC track momentum for well-contained showers from $1.5 < p < 8$ GeV/c electrons identified in the TPC. Uncertainties arise from sensitivity to electron selection cuts, residual hadronic contamination of the electron sample, and the limited statistics of the d+Au data set. We have confirmed the electron calibration by reconstructing the π^0 invariant mass, and anticipate reducing the scale uncertainty for future data.

Figure 2a shows the MB and HT cross section averaged over 2003 and 2004 data versus jet p_T . The MB and HT data are in good agreement for overlapping jet p_T ($\chi^2/\text{ndf} = 1.0$), despite the very different $c(p_T)$. The curve shows the NLO perturbative QCD cross section of Ref. [6] evaluated at equal factorization and renormalization scales, $\mu \equiv \mu_F = \mu_R = p_T$, using the CTEQ6M set of parton distributions [18]. The theoretical cross section changes by less than 23% if μ is varied by a factor of two. It increases by 1% (13%) at p_T of 10 (40) GeV/c if the CTEQ6.1M distributions are used instead. Theory and data are compared in Figure 2b. Satisfactory agreement is found over seven orders of magnitude. The systematic uncertainty amounts to 8% in the normalization with the BBC and 48% in the measured yield, consisting of 5% due to residual beam background, 13% on $c(p_T)$,

and 46% from a 9% uncertainty on the jet energy scale. The latter is dominated by uncertainty on the BEMC calibration and losses of some neutral particles, for example neutrons. No corrections were made for the non-perturbative redistribution of energy into and out of the jet by the underlying event and out-of-cone hadronization. We estimate that their combined effect amounts to $\sim 25\%$ of the differential cross section for $p_T > 10$ GeV/c and improves the agreement between data and theory.

The asymmetry A_{LL} was extracted for $5 < p_T < 17$ GeV/c from the HT data sample of about 110×10^3 jets in 2003 and 210×10^3 in 2004. The larger sample size was obtained by removing the BEMC software energy threshold imposed in the cross section analysis. The jet yields N were sorted by equal (++) and opposite (+-) beam helicity configuration. The asymmetry was extracted as:

$$A_{LL} = \frac{\sum(P_1 P_2)(N^{++} - RN^{+-})}{\sum(P_1 P_2)^2(N^{++} + RN^{+-})} \quad (3)$$

in which $P_{1,2}$ are the measured proton beam polarizations, $R \simeq 1.1$ is the ratio of measured luminosities for equal and opposite proton beam helicities, and parity violating differences $\lesssim \mathcal{O}(10^{-4})$ in the cross sections for different beam helicities are neglected. The sums are performed over runs typically lasting 20 minutes.

The results for A_{LL} from 2003 and 2004 data are in good agreement ($\chi^2/\text{ndf} = 0.3$). Figure 3 shows the combined A_{LL} versus jet p_T , together with the statistical (bars) and systematic (bands) uncertainties.

A 25% combined scale uncertainty arises from the CNI beam polarization measurement (22% in 2003 and an uncorrelated 16% in 2004) and from the CNI absolute calibration (18% common to both years).

The uncertainty in R was estimated to be 0.003 using narrow and wide timing requirements for the BBC coincidence. It takes into account differences in sampling of the longitudinal vertex distribution in the jet analysis and in the relative luminosity measurement, and corresponds to 0.009 uncertainty in A_{LL} . An independent measurement with the Zero Degree Calorimeters (ZDC) [8] gave consistent results to within statistical uncertainties. No double helicity asymmetry of the BBC measurement relative to the ZDC measurement was observed.

Residual non-longitudinal proton beam polarization at the STAR IR could contaminate the A_{LL} measurement through an azimuthally uniform two-spin asymmetry [19]. A limit of 0.010 on such contamination was set from local polarimetry data and from two-spin asymmetry measurements with vertically polarized beams.

Beam background from far upstream sources occasionally caused BEMC signals not associated with collisions at the IR. The effect of such background was reduced with the aforementioned selection on $E_{\text{TPC}}/E_{\text{tot}}$. Residual contributions to reconstructed jet yields were estimated to be no larger than 8% (5%) for the 2003 (2004) data samples by studying the variation of jet spectra with

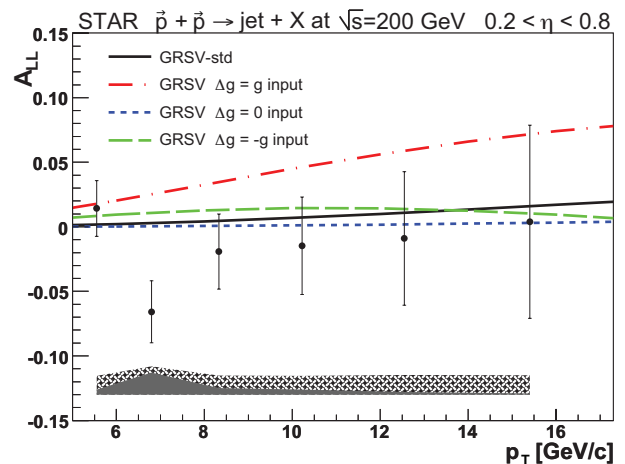


FIG. 3: The longitudinal double-spin asymmetry A_{LL} in $\bar{p} + \bar{p} \rightarrow \text{jet} + X$ at $\sqrt{s} = 200$ GeV versus jet p_T . The uncertainties on the data points are statistical. The gray band indicates the systematic uncertainty from the beam polarization measurement, and the hatched band the total systematic uncertainty. The curves show predictions based on deep-inelastic scattering parametrizations of gluon polarization [6, 18].

beam background conditions monitored by the BBC coincidence rate when filled beam bunches crossed empty bunches at the IR. These, combined with asymmetry estimates from beam-background dominated samples, resulted in an uncertainty estimate of 0.003 in A_{LL} .

The bias towards hard fragmentation processes caused by the HT trigger requirement was simulated. The resulting p_T dependent shift in A_{LL} was estimated to be less than 0.007 with the polarized parton distributions of Ref. [20]. The size of possible biases introduced by jet reconstruction and jet p_T resolution were determined in the same way and found to be less than 0.004. The total bias is estimated to be less than 0.009.

Analyses with randomized proton beam helicity configurations and other cross-checks including parity violating single-spin asymmetries showed no evidence for beam bunch to bunch or fill to fill systematics in A_{LL} .

The curves in Figure 3 show theoretical evaluations [6, 18] at $\mu_F = \mu_R = p_T$ for the commonly used polarized parton distributions of Ref. [20]. The predicted asymmetry shift by less than 0.003 (0.017) at $p_T = 5.6$ (15.7) GeV/c if the scales are varied by a factor of two. The polarized parton distributions are based on a best fit to polarized inclusive DIS data, the so-called GRSV-standard gluon polarization distribution, and on assumptions of (i) a vanishing gluon polarization $\Delta g(x, Q_0^2) = 0$, and (ii) maximally positive or negative gluon polarization, $\Delta g(x, Q_0^2) = \pm g(x, Q_0^2)$, at the initial scale $Q_0^2 = 0.4 \text{ GeV}^2/c^2$ in the analysis [20]. The STAR jet asymmetries are systematically below the $\Delta g(x, Q_0^2) = g(x, Q_0^2)$ evaluation ($\chi^2/\text{ndf} \simeq 3$) and are consistent with the other evaluations, in qualitative agreement with the observa-

tions in Refs. [3, 4, 5]. The results thus disfavor large and positive gluon polarization, proposed [21] originally to explain the small quark spin contribution to the proton spin.

In summary, we report the first measurement of the longitudinal double-spin asymmetry A_{LL} for inclusive jets with transverse jet momenta of $5 < p_T < 17$ GeV/c produced at mid-rapidity in polarized proton collisions at $\sqrt{s} = 200$ GeV. The cross section was determined for $5 < p_T < 50$ GeV/c jets and is described by NLO perturbative QCD evaluations over seven orders of magnitude. The asymmetries A_{LL} are consistent with NLO perturbative QCD calculations utilizing polarized quark and gluon distributions from inclusive deep-inelastic polarized lepton-nucleon scattering analyses, and disfavor large positive values of gluon polarization in the nucleon.

We thank the RHIC Operations Group and RCF at BNL, and the NERSC Center at LBNL for their support. This work was supported in part by the Offices of NP and HEP within the U.S. DOE Office of Science; the U.S. NSF; the BMBF of Germany; CNRS/IN2P3, RA, RPL, and EMN of France; EPSRC of the United Kingdom; FAPESP of Brazil; the Russian Ministry of Science and Technology; the Ministry of Education and the NNSFC of China; IRP and GA of the Czech Republic, FOM of the Netherlands, DAE, DST, and CSIR of the Government of India; Swiss NSF; the Polish State Committee for Scientific Research; SRDA of Slovakia, and the Korea Sci. & Eng. Foundation.

- (2001) and references therein.
- [2] SMC, B. Adeva *et al.*, Phys. Rev. **D58**, 112002 (1998); E155, P. L. Anthony *et al.*, Phys. Lett. **B493**, 19 (2000).
 - [3] HERMES, A. Airapetian *et al.*, Phys. Rev. Lett. **84**, 2584 (2000); SMC, B. Adeva *et al.*, Phys. Rev. **D70**, 012002 (2004); COMPASS, E.S. Ageev *et al.*, Phys. Lett. **B633**, 25 (2006).
 - [4] E581/E704, D.L. Adams *et al.*, Phys. Lett. **B261**, 197 (1991); Phys. Lett. **B336**, 269 (1994).
 - [5] PHENIX, S.S. Adler *et al.*, Phys. Rev. Lett. **93**, 202002 (2004); Phys. Rev. **D73**, 091102(R) (2006).
 - [6] B. Jäger *et al.*, Phys. Rev. **D70**, 034010 (2004).
 - [7] G. Bunce *et al.*, Ann. Rev. Nucl. Part. Sci. **50**, 525 (2000).
 - [8] Special Issue: RHIC and Its Detectors, Nucl. Instrum. Meth. **A499** (2003).
 - [9] O. Jinnouchi *et al.*, RHIC/CAD Note 171 (2004).
 - [10] H. Okada *et al.*, hep-ex/0601001, Phys. Lett. **B**, in press.
 - [11] J. Kiryluk *et al.*, hep-ex/0501072, published in Spin 2004 Conference Proceedings, Trieste, Italy.
 - [12] STAR, J. Adams *et al.*, Phys. Rev. Lett. **91**, 172302 (2003).
 - [13] G. Blazey *et al.*, hep-ex/0005012, published in Batavia 1999, QCD and weak boson physics in RunII.
 - [14] T. Sjostrand *et al.*, Comput. Phys. Commun. **135**, 238 (2001).
 - [15] R.D. Field *et al.*, hep-ph/0510198, CDF-ANAL-CDF-PUBLIC-7822.
 - [16] GEANT 3.21, CERN program library.
 - [17] G. Corcella *et al.*, J. High Energy Phys. 0101, 010 (2001).
 - [18] J. Pumplin *et al.*, J. High Energy Phys. 0207, 012 (2002).
 - [19] H. Mayer *et al.*, Phys. Rev. Lett. **81**, 3096 (1998).
 - [20] M. Glück *et al.*, Phys. Rev. **D63**, 094005 (2001).
 - [21] G. Altarelli and G.G. Ross, Phys. Lett. **B212**, 391 (1988); R.D. Karlitz *et al.*, Phys. Lett. **B214**, 229 (1988).

[1] EMC, J. Ashman *et al.*, Nucl. Phys. **B328**, 1 (1989); B.W. Filippone and X.D. Ji, Adv. Nucl. Phys. **26**, 1